

## Effective interactions between the N-H bond orientations in lithium imide and a proposed ground-state structure

Tim Mueller and Gerbrand Ceder\*

*Department of Materials Science and Engineering, Massachusetts Institute of Technology, Building 13-5056, 77 Massachusetts Avenue, Cambridge, Massachusetts 02139, USA*

(Received 28 February 2006; revised manuscript received 17 July 2006; published 4 October 2006)

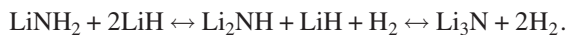
Lithium imide ( $\text{Li}_2\text{NH}$ ) is a candidate material for hydrogen storage but its structure has proven difficult to fully characterize. The key problem is to identify the location of the hydrogen positions and N-H bond orientations in the structure. By searching an effective Hamiltonian in which the energy of lithium imide is expressed as a function of imide group orientations it is shown that nearest-neighbor imide groups prefer to orient antiparallel within a  $\{110\}$  plane of the antifluorite host structure. Although this orientation is frustrated in the antifluorite structure we suggest a ground state for  $\text{Li}_2\text{NH}$  which has the lowest energy of any known structure as calculated by density functional theory.

DOI: [10.1103/PhysRevB.74.134104](https://doi.org/10.1103/PhysRevB.74.134104)

PACS number(s): 61.50.Ah, 61.66.Fn, 71.15.Nc, 71.20.Ps

### I. INTRODUCTION

The ground-state structure of lithium imide ( $\text{Li}_2\text{NH}$ ) is not fully known. While general agreement exists that the average positions of the Li and N atoms form an antifluorite structure, very different assignments of the H positions have been proposed.<sup>1-6</sup> Establishing the details of this structure has become more relevant with the observations of Chen *et al.*<sup>7</sup> that the combination of lithium amide ( $\text{LiNH}_2$ ) and lithium hydride ( $\text{LiH}$ ) releases hydrogen in a two-step reaction:



The first step in this reaction, in which lithium amide reacts with lithium hydride to form lithium imide ( $\text{Li}_2\text{NH}$ ), is of interest as a hydrogen storage system because it releases up to 6.5 wt. % hydrogen and is reversible at temperatures below 300 °C.<sup>7</sup> The structures of lithium amide and lithium hydride are well characterized, but despite the recent high levels of interest in lithium imide a consensus on a complete specification of its structure remains lacking. The distinction between structural models is significant, as recent *ab initio* calculations indicate that the energy of the imide depends rather strongly on the H positions.<sup>3,5,6</sup> Hence a good structural model and insight into the factors that determine the arrangement of hydrogen nuclei in these imides is required. In this paper we develop a model to obtain the *effective* H-H interaction in Li imide and use it to obtain a structure with lower energy than any previously proposed structure.

Using x-ray diffraction, Juza and Opp concluded that lithium imide is most likely antifluorite with lithium cations and nitrogen anions, but they were unable to resolve the positions of the hydrogen ions.<sup>8</sup> Several studies since have indicated that each hydrogen nucleus is bonded to a nitrogen nucleus to form an imide (N-H) anion<sup>1-6</sup> though the orientation of these N-H groups is unknown. Using neutron powder diffraction (NPD), Ohoyama *et al.* proposed a structure in which hydrogen randomly occupies one of four symmetrically equivalent sites around the nitrogen ion.<sup>1</sup> Based on synchrotron x-ray diffraction results, Noritake *et al.* supported another structure, in which the hydrogen randomly occupies one of twelve sites around the nitrogen ion.<sup>2</sup> Zhang *et al.*

treated the hydrogen nucleus as a quantum mechanical particle and found that when nitrogen and lithium ions are fixed at their antifluorite positions the wave function of a hydrogen nucleus is centered at the nitrogen nucleus with density maxima along the  $\langle 100 \rangle$  directions.<sup>4</sup>

Herbst and Hector, based on experimental work by Balogh *et al.*<sup>5</sup> and density functional theory<sup>9</sup> (DFT) calculations, have proposed a fully occupied low-symmetry structure in which one in eight lithium ions have moved to the empty octahedral sites between nitrogen ions.<sup>3</sup> They calculated the enthalpy of formation of their proposed structure to be approximately 17 to 38 kJ per mol formula unit (f.u.) higher than the experimentally derived enthalpy of formation for lithium imide, as opposed to a difference of 3 kJ per mol f.u. for  $\text{LiNH}_2$ .<sup>3</sup> This suggests that although the structure they propose produces diffraction patterns similar to those observed experimentally it may not be the energetic ground state. Very recently Magyari-Köpe *et al.* discovered several structures with significantly lower calculated energies than any previously suggested structure.<sup>6</sup>

It is worth considering whether lithium imide might be thermally disordered at room temperature. Ohoyama *et al.* find no evidence of a structural phase transition between 10 K and room temperature,<sup>1</sup> suggesting that if the structure is disordered at room temperature the disorder persists to a very low temperature. A differential thermal analysis (DTA) study of lithium imide indicates that there is a second-order phase transition at about 356 K, which has been attributed to an order-disorder transition.<sup>10</sup> Balogh *et al.* have found a similar result.<sup>5</sup> These results suggest that the hydrogen positions in lithium imide are fully or partially ordered at room temperature.

Kojima and Kawai have shown that lithium imide shows two broad N-H stretching peaks in the infrared, unlike lithium amide for which the absorption peaks are sharp.<sup>11</sup> Although the authors suggest that the peak broadening could be due to small crystallite size or thermal disorder, their results might also indicate a wide variety of local environments for N-H groups, implying either partial disorder or a large unit cell for the imide.

The challenge in determining the ground-state structure of lithium imide is primarily one of determining the lowest-

energy orientations for the imide groups. The N-H bond length varies little; its average length in 99 relaxed structures calculated for this paper is 1.038 Å and the standard deviation is 0.003 Å. However the orientation of one N-H bond substantially affects the orientations of N-H bonds in neighboring cells. To perform a thorough search of possible ground states and to clarify the interaction between N-H bond orientations we develop an effective Hamiltonian for N-H bond orientations in lithium imide. The objective is to write the energy of the system directly in terms of the orientation of the N-H groups with the other degrees of freedom implicitly minimized over. The model is parametrized with *ab initio* calculations and used to predict a structure with lower calculated energy than any structure known to date.

## II. METHODOLOGY

The effective Hamiltonian for the N-H orientations is based on a modification of the cluster expansion<sup>12,13</sup> formalism to include continuous variables describing the imide group orientation. The N-H bond orientation on the  $i$ th imide group can be characterized with a polar and azimuthal coordinate,  $(\theta_i, \phi_i)$ . The objective of our model is to find an expression for the function

$$F(\theta_1, \phi_1, \theta_2, \phi_2, \theta_3, \phi_3, \dots), \quad (1)$$

where  $F$  is the energy of the system with the N-H groups in the specified orientations, and with all other coordinates relaxed (e.g., the N-H bond length and the Li positions). This coarse-grained energy function is similar to the cluster expansion for configurational disorder in alloy theory where displacements (and sometimes vibrations) are coarse grained over to obtain an energy expression solely in terms of site occupation variables.<sup>12-14</sup>

For each domain  $(\theta_i, \phi_i)$  we define a local basis of functions  $f_{n_i}(\theta_i, \phi_i)$ , where  $f_{n_i}$  indicates the  $n$ th basis function for the  $i$ th imide group. The tensor product of these local bases forms a basis for the function  $F$ ,

$$F(\theta_1, \phi_1, \dots) = \sum_{\vec{n}} \left( V_{\vec{n}} \prod_i f_{n_i}(\theta_i, \phi_i) \right),$$

where  $\vec{n}$  is a vector of basis function indices in which the  $i$ th element is  $n_i$ . The sum is over all possible  $\vec{n}$ , and  $V_{\vec{n}}$  are coefficients to be determined later.

For example, if  $F$  is square integrable over imide group orientations,  $f_{n_i}$  can be chosen as spherical harmonics. As with a discrete cluster expansion, it is convenient to choose  $f_{n_i}$  such that  $f_{0_i}$  is a constant for all  $i$ . The function  $F$  can then be expanded as a linear combination of functions of the orientations of single imide groups, functions of the orientations of pairs of imide groups, etc.,

$$\begin{aligned} F(\theta_1, \phi_1, \dots) = & V_0 + \sum_i \sum_{n_i \neq 0} V_{n_i} f_{n_i}(\theta_i, \phi_i) \\ & + \sum_{i,j} \sum_{n_i \neq 0, n_j \neq 0} V_{n_i n_j} f_{n_i}(\theta_i, \phi_i) f_{n_j}(\theta_j, \phi_j) + \dots \end{aligned} \quad (2)$$

The symmetry properties of the crystal can be used to group terms that share the same coefficient. Hence, it is more convenient to choose basis functions  $f_{n_i}$  that form closed orbits under the operations in the space group of the crystal. One result of this step is that terms that are antisymmetric with respect to the symmetry operations of the crystal disappear.

The expansion in Eq. (2) is in principle an exact representation of Eq. (1), but to reduce this to a finite problem it is necessary to make approximations based on physical intuition. As with a discrete cluster expansion, we assume that Eq. (2) will be dominated by the constant term and terms representing the interactions between physically small clusters of imide groups. In this paper, we include only terms representing single imide groups and imide pair interactions up to the next-next-nearest neighbor.

For continuous domains there are an infinite number of basis functions  $f_{n_i}$  in the complete basis. In practice we include only the basis functions that should have the most physical relevance. For example, for a basis of spherical harmonics one might truncate the basis at a certain angular momentum. For lithium imide we have generated a truncated basis from hybridized spherical harmonics,

$$f_{0_i} = 1,$$

$$f_{1_i} = \frac{1}{2} \sqrt{30} x_i y_i,$$

$$f_{2_i} = \frac{1}{2} \sqrt{210} x_i y_i z_i,$$

$$f_{3_i} = \frac{1}{4} [\sqrt{175} x_i^3 - \sqrt{63} x_i + \sqrt{105} x_i (y_i^2 - z_i^2)],$$

$$f_{4_i} = \frac{5}{8} \sqrt{7} (x_i^4 + y_i^4 + z_i^4) + \frac{1}{2} \sqrt{\frac{5}{6}} (3x_i^2 - 1) + \frac{1}{2} \sqrt{3} x_i - \frac{3}{8} \sqrt{7},$$

where  $x_i = \cos \theta_i \sin \phi_i$ ,  $y_i = \sin \theta_i \sin \phi_i$ , and  $z_i = \cos \phi_i$ . The full truncated basis used can be generated by applying the cubic symmetry operations to these functions and keeping the ones that are linearly independent.

To determine the coefficients  $V_n$  of this expansion we calculated a library of 98 relaxed structures with different relative N-H orientations using the projector augmented wave function.<sup>15</sup> (PAW) method with the Perdew-Burke-Eznerhof<sup>16</sup> (PBE) generalized gradient approximation (GGA) to DFT as implemented in the Vienna *ab initio* simulation package (VASP).<sup>17</sup> The standard hydrogen and nitrogen PAW potentials and  $s$ -valence Li PAW potentials in VASP were used with a plane wave cutoff energy of 520 eV. Calculations were considered converged when forces reached less than 80 meV/Å. For a primitive cell calculation, total energy convergence within 1 meV per formula unit was reached with a  $7 \times 7 \times 7$  Monkhorst-Pack<sup>18</sup>  $k$ -point grid shifted to include the  $\gamma$  point. For supercell calculations this grid was scaled down proportionately to the size of the supercell. The coefficients were evaluated using a least-

squares regression. To help prevent overfitting the coefficients were fit to both the energies in eV per formula unit and the forces in eV/Å, with the energies given ten times the weight of the forces. To more accurately represent low-energy interactions, structures with lower energy were assigned higher weights. To ensure the cluster expansion had predictive power a Metropolis algorithm<sup>19</sup> was used to find a subset of terms in the expansion that had a low leave-one-out cross-validation score.<sup>20</sup> The coefficients for this model generated from the original library of 98 structures and the new-found orthorhombic structure are given in Table I.

The enthalpies of formation of several low-energy structures were calculated. To ensure accurate results the electronic energies were recalculated using hard hydrogen and nitrogen PAW potentials and the cutoff energy was increased to 900 eV. Calculations were considered converged when the forces on the ions were less than 1 meV/Å. Vibrations within the harmonic approximation were evaluated within the linear response approach as implemented in ABINIT<sup>21</sup> with the PBE GGA exchange-correlation functional. The Fritz-Haber Institute pseudopotentials provided with ABINIT were used, and the cutoff energy was 35 Ry. For the electronic supercell calculations a  $4 \times 4 \times 4$   $k$ -point grid including the  $\gamma$  point was used, and interatomic forces were calculated on a  $2 \times 2 \times 2$  grid. For the layered structure a  $6 \times 6 \times 6$  electronic  $k$ -point grid and  $3 \times 3 \times 3$  interatomic force grid were used. Ideal gas behavior was assumed for the standard state of the reference molecules  $H_2$  and  $N_2$ . The values for  $H_2$  and  $N_2$  reference molecules were calculated in cubic cells with length 15 Å. It was found that increasing the size of the cell to 17 Å changed the calculated energies by less than 0.01 meV.

### III. RESULTS

Within our model, the interaction between a single pair of nearest-neighbor imide groups is represented by

$$\begin{aligned} & \sum_{n_1 \neq 0} V_{n_1} f_{n_1}(\theta_1, \phi_1) + \sum_{n_2 \neq 0} V_{n_2} f_{n_2}(\theta_2, \phi_2) \\ & + \sum_{n_1 \neq 0, n_2 \neq 0} V_{n_1, n_2} f_{n_1}(\theta_1, \phi_1) f_{n_2}(\theta_2, \phi_2), \end{aligned} \quad (3)$$

where we have included the contributions from single-imide terms.

The minimum of Eq. (3) represents the most favorable nearest-neighbor imide group orientations and can be visualized in Fig. 1(a). This interaction will be referred to as the “preferred” nearest-neighbor orientation. Similar to the observation made in Ref. 6, we find that neighboring imide groups tend to align antiparallel to one another. The nitrogen and hydrogen nuclei are coplanar with the two lithium nuclei between the imide groups in the  $(1\bar{1}0)$  plane, and a N-N-H bond angle of  $36.3^\circ$ . The hydrogen nucleus on each group tilts towards the nitrogen of the other group, possibly to form a hydrogen bond. In practice the apparent unfavorable proximity between the hydrogen ions and the lithium ions between groups is resolved as these lithium ions move towards nearby empty octahedral sites. We find only relaxation *to-*

*wards* octahedral sites unlike the full displacement suggested in Ref. 3.

It is impossible for a single imide group to be in the preferred orientation with more than one of its nearest neighbors. To see this, let one imide group, “group A,” be in the preferred orientation with a nearest-neighbor imide group, “group B,” with the vector from group A to group B in the  $[110]$  direction. Let group B be oriented such that it is at an angle of  $1.1^\circ$  to the  $[\bar{1}\bar{1}1]$  direction [Fig. 1(a)]. All ways in which group B can be in the preferred orientation with any of its nearest neighbors can be generated by applying the 48 fcc point symmetry operations at group B to imide groups A and B. It is only possible for imide group B to be in the preferred orientation with two different imide groups simultaneously if an operation leaves the orientation of group B unchanged but maps group A onto a different nearest neighbor. The only operation that results in group B having the exact same orientation is reflection about the  $(1\bar{1}0)$  plane, but this maps group A onto itself. This frustration can be partially resolved if the N-H bonds rotate slightly so that they are aligned in the high-symmetry  $[\bar{1}\bar{1}1]$  direction [Fig. 1(b)]. This is still a low-energy orientation because of the ability for the lithium ions to relax towards the empty octahedral sites. We will refer to this as the near-preferred orientation. If groups A and B are in the near-preferred orientation, the symmetry operations corresponding to  $120^\circ$  rotations about the  $[\bar{1}\bar{1}1]$  axis all map the orientation of group B onto itself, but maps group A onto three different nearest neighbors. This allows group B to be in the near-preferred orientation relative to three nearest neighbors at the same time (Fig. 2). For every imide group to be in the near-preferred orientation relative to three nearest neighbors, the structure must consist of  $\{111\}$  planes of alternating antiparallel imide groups where the imide groups in each plane are aligned orthogonally to the plane. This structure, after relaxation with DFT, becomes the one shown in Fig. 3. Nuclear coordinates for the relaxed structure, which will be referred to as the “layered” structure, are given in Table II.

In addition to providing insight into the effective N-H interactions, the cluster expansion can also be used to very rapidly search for low-energy structures of lithium imide. A search for the ground state of this model was performed with Monte Carlo simulation in all supercells up to eight formula units. The lowest energy configuration is shown in Fig. 4(a). A DFT calculation relaxes this structure to the one shown in Fig. 4(b), which will be referred to as the “orthorhombic” structure. This structure, although not in the initial library of structures used to fit the coefficients, was added when determining the preferred orientations. The lithium ions in the relaxed structure have moved significantly from their ideal antifuorite positions. The new structure has an orthorhombic unit cell, with coordinates given in Table III and calculated lattice parameters of 5.12, 10.51, and 5.27 Å, although these are probably overestimated by a few percent as is typical in the GGA approximation.<sup>22–24</sup> The space group of the structure as determined by ABINIT is Pbcu (#61). Every imide group in this structure is involved in a nearest-neighbor pair interaction resembling the preferred nearest-neighbor orien-

TABLE I. The parameters for the model Hamiltonian. Each row lists a sample term from an included orbit of functions and the coefficient for functions in that orbit. The imide groups for the sample functions, in conventional antiferroite reduced coordinates, are located at (0,0,0) for site 1 and (0.5,0.5,0) for site 2 for nearest neighbors, (0,0,0) and (1,0,0) for next-nearest neighbors, and (0,0,0) and (1,0.5,0.5) for next-next-nearest neighbors. The functions are  $f_1(a,b)=\frac{1}{2}\sqrt{3}0ab$ ,  $f_2(a,b,c)=\frac{1}{2}\sqrt{2}10abc$ ,  $f_3(a,b,c)=\frac{1}{4}[\sqrt{175}a^3-\sqrt{63}a+\sqrt{105}a(b^2-c^2)]$ , and  $f_4(a)=\frac{5}{8}\sqrt{7}(x^4+y^4+z^4)+\frac{1}{2}\sqrt{\frac{5}{6}}(3a^2-1)+\frac{1}{2}\sqrt{3}a-\frac{3}{8}\sqrt{7}$ . All functions symmetrically equivalent to those listed were included in the Hamiltonian.

Cluster	Site 1 function	Site 2 function	Terms per formula unit	$V_n$ (kJ/mol f. u.)	$V_n$ (meV/mol f. u.)
Empty	1	1	1	-179.73607	-1862.78463
Point	$f_4(-x)$	1	6	0.91880	9.52246
Nearest neighbor	$f_1(x,y)$	$f_1(x,y)$	6	0.38115	3.95020
	$f_1(x,y)$	$f_4(x)$	24	0.04595	0.47620
	$f_1(x,y)$	$f_3(x,z,y)$	24	0.01690	0.17514
	$f_1(x,z)$	$f_1(y,z)$	12	0.11320	1.17316
	$f_1(x,z)$	$f_4(-z)$	48	-0.06256	-0.64833
	$f_2(x,y,z)$	$f_2(x,y,z)$	6	0.31453	3.25979
	$f_2(x,y,z)$	$f_4(-z)$	24	-0.08269	-0.85699
	$f_2(x,y,z)$	$f_3(z,y,x)$	24	-0.05846	-0.60589
	$f_4(-x)$	$f_4(-x)$	24	-0.07591	-0.78672
	$f_4(-x)$	$f_4(-y)$	24	0.18900	1.95885
	$f_4(-x)$	$f_3(y,x,z)$	24	0.06545	0.67832
	$f_4(-z)$	$f_4(-z)$	12	0.33858	3.50904
	$f_4(-z)$	$f_4(z)$	12	-0.35140	-3.64189
	$f_4(-z)$	$f_3(x,y,z)$	48	-0.03802	-0.39408
	$f_4(-z)$	$f_3(z,y,x)$	48	-0.11254	-1.16640
	$f_4(x)$	$f_3(y,x,z)$	24	-0.09816	-1.01732
	$f_3(x,z,y)$	$f_3(x,z,y)$	12	0.16971	1.75887
	$f_3(x,z,y)$	$f_3(y,x,z)$	24	-0.05320	-0.55134
	$f_3(x,y,z)$	$f_3(x,y,z)$	12	-0.09459	-0.98028
	Next-nearest neighbor	$f_1(x,y)$	$f_1(x,y)$	6	-0.17086
$f_1(x,y)$		$f_4(-y)$	24	-0.04874	-0.50514
$f_1(x,y)$		$f_3(y,x,z)$	12	-0.05271	-0.54629
$f_1(y,z)$		$f_1(y,z)$	3	0.24773	2.56743
$f_1(y,z)$		$f_2(x,y,z)$	6	0.07267	0.75319
$f_4(-y)$		$f_4(-x)$	24	0.21403	2.21818
$f_4(-y)$		$f_4(-y)$	12	0.16783	1.73940
$f_4(-y)$		$f_3(x,y,z)$	24	0.11144	1.15501
$f_3(x,z,y)$		$f_3(x,z,y)$	6	0.06158	0.63821
$f_3(y,z,x)$		$f_3(y,z,x)$	6	-0.13240	-1.37220
Next-nearest neighbors	$f_1(x,y)$	$f_2(x,y,z)$	48	-0.01022	-0.10591
	$f_1(x,y)$	$f_4(-x)$	48	-0.06696	-0.69393
	$f_1(x,y)$	$f_4(-z)$	48	-0.02955	-0.30624
	$f_1(x,y)$	$f_4(z)$	48	-0.02770	-0.28705
	$f_1(x,y)$	$f_3(x,z,y)$	48	-0.03402	-0.35262
	$f_1(x,y)$	$f_3(y,z,x)$	48	-0.03412	-0.35366
	$f_1(x,y)$	$f_3(z,x,y)$	48	0.03978	0.41224
	$f_1(y,z)$	$f_1(y,z)$	12	-0.10254	-1.06277
	$f_1(y,z)$	$f_4(x)$	24	0.02594	0.26880
	$f_2(x,y,z)$	$f_3(y,z,x)$	48	-0.03278	-0.33972
	$f_4(-x)$	$f_4(-y)$	48	-0.05105	-0.52904

TABLE I. (Continued.)

Cluster	Site 1 function	Site 2 function	Terms per formula unit	$V_n$ (kJ/mol f. u.)	$V_n$ (meV/mol f. u.)
	$f_4(-x)$	$f_3(y, z, x)$	48	-0.02563	-0.26559
	$f_4(-y)$	$f_4(-x)$	48	0.06118	0.63411
	$f_4(-y)$	$f_4(y)$	24	-0.23445	-2.42980
	$f_4(-y)$	$f_3(x, y, z)$	48	0.06373	0.66049
	$f_4(-y)$	$f_3(y, x, z)$	48	0.05022	0.52049
	$f_4(x)$	$f_4(-x)$	12	-0.07956	-0.82452
	$f_4(x)$	$f_3(y, x, z)$	48	0.02032	0.21061
	$f_4(x)$	$f_3(y, z, x)$	48	0.04955	0.51353
	$f_4(y)$	$f_4(-z)$	24	0.10778	1.11707
	$f_4(y)$	$f_3(x, z, y)$	48	0.02108	0.21842
	$f_4(y)$	$f_3(z, y, x)$	48	-0.06593	-0.68325
	$f_4(y)$	$f_3(z, x, y)$	48	-0.02153	-0.22311
	$f_3(x, z, y)$	$f_3(x, y, z)$	24	0.03629	0.37610
	$f_3(x, z, y)$	$f_3(y, x, z)$	48	0.01857	0.19244
	$f_3(x, z, y)$	$f_3(y, z, x)$	48	-0.03569	-0.36987
	$f_3(y, x, z)$	$f_3(z, y, x)$	48	-0.03856	-0.39968
	$f_3(y, x, z)$	$f_3(z, x, y)$	24	0.05823	0.60350
	$f_3(y, z, x)$	$f_3(z, y, x)$	24	-0.02714	-0.28129

tation, although the imide groups are rotated  $25.4^\circ$  from the preferred nearest-neighbor orientations to be in the low symmetry  $[0.79, 0.58, 0.20]$  and equivalent directions. The existence of nearest-neighbor orientations similar to the preferred orientation suggests that preference for this type of nearest-neighbor orientation remains high even in an infinite crystal.

We have calculated the formation energies for the layered and orthorhombic structures and the lowest-energy structures proposed in Refs. 3 and 6. We show in Table IV the results of these calculations. The calculated energy of formation for the

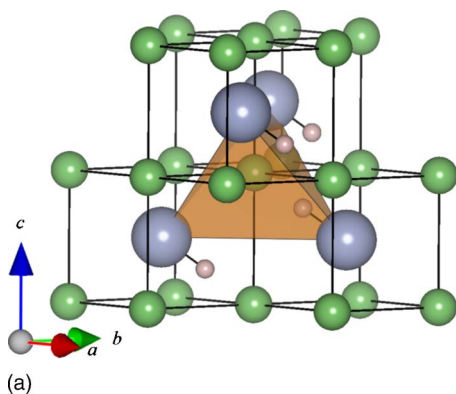


FIG. 1. (Color online) (a) The “preferred” nearest-neighbor orientation. The lithium ions are shown in the ideal antifluorite positions for reference. Both N-H bonds are in the  $(1\bar{1}0)$  plane, which is shown. (b) The more high-symmetry “near-preferred” nearest-neighbor orientation in which the N-H bonds are aligned along  $[\bar{1}\bar{1}1]$  in the  $(1\bar{1}0)$  plane. Dotted lines indicate the lithium ions to which the N-H bonds point. Large spheres represent nitrogen, medium represent lithium, and small represent hydrogen.

new orthorhombic structure is significantly lower than that of any other known low-energy structure.

#### IV. DISCUSSION

Given that it has both the lowest energy known to date in the cluster expansion model, and with GGA, the orthorhombic structure we propose seems like a reasonable candidate for the ground state of lithium imide. The density of this structure, 0.028 formula units per  $\text{\AA}^3$ , is approximately 8% to 10% lower than the experimentally derived density for lithium imide.<sup>1,2,5</sup> A portion of this density difference is likely due to the use of GGA, which typically overestimates

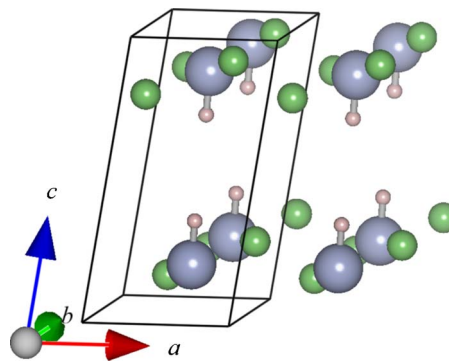


FIG. 2. (Color online) A tetrahedron of nearest-neighbor imide groups. The lower right group is in the near-preferred nearest-neighbor orientation with each of the other three groups, but as a result these groups are not in the near-preferred orientation with each other. Large spheres represent nitrogen, medium represent lithium, and small represent hydrogen.

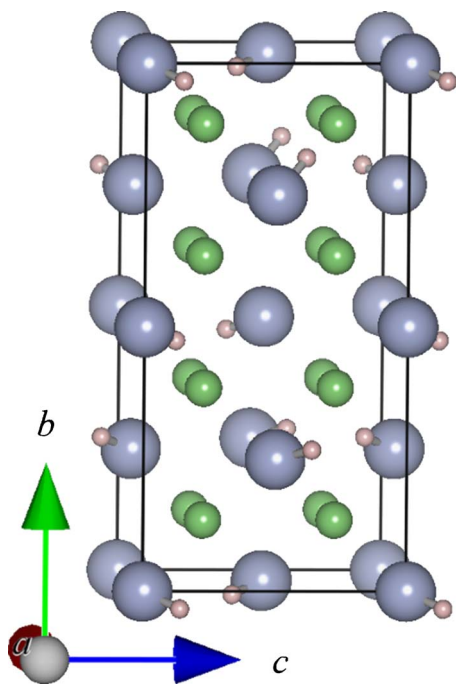


FIG. 3. (Color online) A  $2 \times 2 \times 1$  supercell of the layered structure with the unit cell highlighted. Large spheres represent nitrogen, medium represent lithium, and small represent hydrogen.

the lattice parameter of materials by 1 to 2 percent.<sup>22–24</sup> More significant is the fact that this structure has different symmetry than that indicated by diffraction studies.<sup>1,2,5</sup> There may be several reasons for this discrepancy:

(1) While our search was extensive it is not exhaustive, and it is possible that structures with even lower energy exist which are in better agreement with the experimentally measured diffraction pattern. It is possible that we did not find these because of the limits on our search space or the limits of the model Hamiltonian with which we looked for candidate structures. We want to stress however that the accuracy of the model Hamiltonian does not affect the statement that the orthorhombic structure is lower in energy than all previously suggested structures as that comparison is based on the complete GGA calculation. Because the nearest-neighbor interactions and their topology in the fluorite structure lead to some frustration, it is possible that more complex ordering patterns with larger unit cells have even lower energy as often is the case for frustrated systems.

(2) It is possible that the experimentally observed structure is not the energetic ground state but is stabilized by

TABLE II. The reduced coordinates of the layered structure. All atoms are at Wyckoff position  $2i$  for space group #2 (P-1).  $a = 3.57 \text{ \AA}$ ,  $b = 3.58 \text{ \AA}$ ,  $c = 6.80 \text{ \AA}$ ,  $\alpha = 77.83^\circ$ ,  $\beta = 82.23^\circ$ , and  $\gamma = 59.91^\circ$ .

Atom	$X$	$Y$	$Z$
Lithium	0.980	0.405	0.258
Lithium	0.674	0.202	0.905
Nitrogen	0.653	0.090	0.203
Hydrogen	0.364	0.956	0.640

TABLE III. The reduced coordinates of the orthorhombic structure. All atoms are at Wyckoff position  $8c$  for space group #61 (Pbca).  $a = 5.12 \text{ \AA}$ ,  $b = 10.51 \text{ \AA}$ , and  $c = 5.27 \text{ \AA}$ .

Atom	$X$	$Y$	$Z$
Lithium	0.372	0.540	0.651
Lithium	0.480	0.256	0.191
Nitrogen	0.297	0.370	0.451
Hydrogen	0.363	0.610	0.066

equilibrium finite-temperature entropy effects that are not captured by the harmonic approximation.

(3) It is possible that the experimentally observed structure is not the energetic ground state, but may be instead a higher-symmetry metastable state with some level of frozen-in disorder. This state may be a partially disordered variation of the structure proposed in this paper, or it may be an entirely different structure.

(4) It is possible that GGA or the approach of treating hydrogen classically is not accurate enough for this material.

Better agreement with experiment might be achieved by determining a more complete solution of the hydrogen nuclear wave function. Even at low temperatures there may be rapid tunneling of the hydrogen atoms between low-energy sites, similar to that proposed by Zhang *et al.*<sup>4</sup> The potential energy surface of one hydrogen nucleus is affected

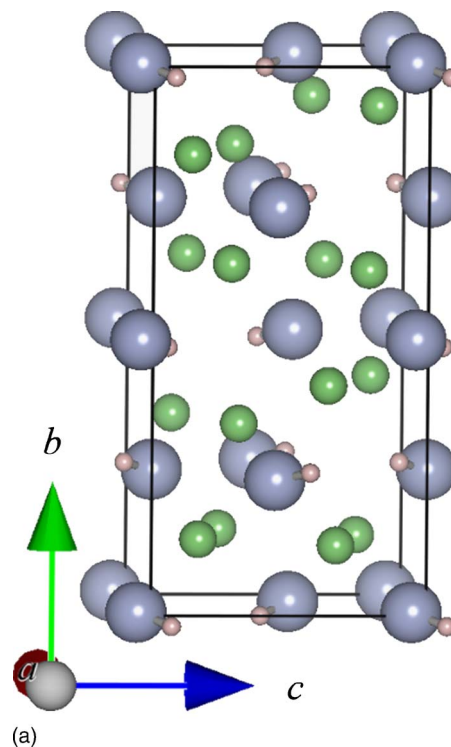


FIG. 4. (Color online) (a) The imide group orientations with the lowest predicted energy after searching structures with up to eight formula units per unit cell. Lithium ions are shown in the ideal antiferro sites for reference. (b) The structure after relaxation with density functional theory. Large spheres represent nitrogen, medium represent lithium, and small represent hydrogen.

TABLE IV. The calculated electronic and total formation energies and vibrational energies for the structures proposed in Refs. 3 and 6 and the layered and orthorhombic structures presented in this paper. The values are given in kJ/mol f. u. (eV/mol f. u.).

Structure	$\Delta E_{\text{electronic}}$	$E_{\text{vibration}}$		$\Delta E_{\text{total}}$	
		0 K	298.2 K	0 K	298.2 K
Ref. 3	-183.5 (-1.902)	46.7 (0.484)	56.6 (0.587)	-166.3 (-1.724)	-173.6 (-1.799)
Ref. 6	-186.6 (-1.934)	47.5 (0.492)	56.9 (0.590)	-168.6 (-1.748)	-176.4 (-1.829)
Layered structure	-186.3 (-1.931)	47.0 (0.487)	56.3 (0.584)	-168.8 (-1.750)	-176.7 (-1.831)
Orthorhombic structure	-188.3 (-1.952)	47.2 (0.489)	56.6 (0.587)	-170.7 (-1.769)	-178.4 (-1.849)

by location of nearby nuclei, so we believe it is likely that any motion of hydrogen ions is locally correlated and dependent on lithium and nitrogen positions at low temperatures.

In summary, we have developed a model to express the formation energy of lithium imide as a function of the orientations of imide groups and used this model to identify low-energy interactions between nearby imide groups. Our results in conjunction with previous studies<sup>1-6</sup> point at the difficulty in predicting the ground state of lithium imide and of materials in general.<sup>25</sup> Our model predicts the existence of a structure that has been confirmed to have a lower energy, as determined by DFT, than any known structure. Although this model has been applied to the formation energy of lithium

imide in this paper, we believe that the general approach of expanding local interactions between nuclear coordinates can be used to model the properties of a variety of materials.

#### ACKNOWLEDGMENTS

This work was funded by the Army Research Office through the Institute for Soldier Nanotechnologies under Grant No. DAAD19-02-D-0002, and the Department of Energy under Contract No. DE-FG02-05ER46253. Supercomputing resources from the San Diego Supercomputing Center are acknowledged.

\*Author to whom correspondence should be addressed. FAX: (617) 258-6534. Email address: gceder@mit.edu

<sup>1</sup>K. Ohoyama, Y. Nakamori, S. Orimo, and K. Yamada, *J. Phys. Soc. Jpn.* **74**, 483 (2005).

<sup>2</sup>T. Noritake, H. Nozaki, M. Aoki, S. Towata, G. Kitahara, Y. Nakamori, and S. Orimo, *J. Alloys Compd.* **393**, 264 (2005).

<sup>3</sup>J. F. Herbst and L. G. Hector, Jr., *Phys. Rev. B* **72**, 125120 (2005).

<sup>4</sup>C. J. Zhang, M. Dyer, and A. Alavi, *J. Phys. Chem. B* **109**, 22089 (2005).

<sup>5</sup>M. P. Balogh, C. Y. Jones, J.F. Herbst, L. G. Hector, Jr., and M. Kundrat, *J. Alloys Compd.* **420**, 326 (2006).

<sup>6</sup>B. Magyari-Köpe, V. Ozolins, and C. Wolverton, *Phys. Rev. B* **73**, 220101 (2006).

<sup>7</sup>P. Chen, Z. T. Xiong, J. Z. Luo, J. Y. Lin, and K. L. Tan, *Nature (London)* **420**, 302 (2002).

<sup>8</sup>R. Juza and K. Opp, *Z. Anorg. Allg. Chem.* **266**, 325 (1951).

<sup>9</sup>W. Kohn and L. J. Sham, *Phys. Rev.* **140**, 1133 (1965).

<sup>10</sup>R. A. Forman, *J. Chem. Phys.* **55**, 1987 (1971).

<sup>11</sup>Y. Kojima and Y. Kawai, *J. Alloys Compd.* **395**, 236 (2005).

<sup>12</sup>D. de Fontaine, in *Solid State Physics*, edited by D. Turnbull and F. Seitz (Academic Press, New York, 1979), Vol. 34, p. 73.

<sup>13</sup>J. M. Sanchez, F. Ducastelle, and D. Gratias, *Physica A* **128**, 334 (1984).

<sup>14</sup>G. Ceder, *Curr. Opin. Solid State Mater. Sci.* **6**, 533 (1998).

<sup>15</sup>P. E. Blochl, *Phys. Rev. B* **50**, 17953 (1994).

<sup>16</sup>J. P. Perdew, K. Burke, and M. Ernzerhof, *Phys. Rev. Lett.* **77**, 3865 (1996).

<sup>17</sup>G. Kresse and J. Furthmüller, *Phys. Rev. B* **54**, 11169 (1996).

<sup>18</sup>H. J. Monkhorst and J. D. Pack, *Phys. Rev. B* **13**, 5188 (1976).

<sup>19</sup>N. Metropolis, A. Rosebluth, M. Rosebluth, and A. Teller, *J. Chem. Phys.* **21**, 1087 (1953).

<sup>20</sup>A. Van de Walle and G. Ceder, *J. Phase Equilib.* **23**, 348 (2002).

<sup>21</sup>X. Gonze, J. M. Beuken, R. Caracas, F. Detraux, M. Fuchs, G. M. Rignanese, L. Sindic, M. Verstraete, G. Zerah, F. Jollet, M. Torrent, A. Roy, M. Mikami, P. Ghosez, J. Y. Raty, and D. C. Allan, *Comput. Mater. Sci.* **25**, 478 (2002).

<sup>22</sup>M. Korling and J. Haglund, *Phys. Rev. B* **45**, 13293 (1992).

<sup>23</sup>M. Fuchs, M. Bockstedte, E. Pehlke, and M. Scheffler, *Phys. Rev. B* **57**, 2134 (1998).

<sup>24</sup>M. Fuchs, J. L. F. DaSilva, C. Stampfl, J. Neugebauer, and M. Scheffler, *Phys. Rev. B* **65**, 245212 (2002).

<sup>25</sup>C. C. Fischer, K. J. Tibbetts, D. Morgan, and G. Ceder, *Nat. Mater.* **5**, 641 (2006).